This is a repository copy of *Synthesis and Characterisation of Fused-Heterocyclic Molecular Rods: A Combined Experimental and Theoretical Study on Diethynyl-Dithienothiophenyl Derivatives*.

White Rose Research Online URL for this paper:
http://eprints.whiterose.ac.uk/119239/

Version: Accepted Version

Article:

Jones, L orcid.org/0000-0001-6657-2632, Pask, CM orcid.org/0000-0002-2241-5069, Kazlauciunas, A et al. (2 more authors) (2017) Synthesis and Characterisation of Fused-Heterocyclic Molecular Rods: A Combined Experimental and Theoretical Study on Diethynyl-Dithienothiophenyl Derivatives. ChemistrySelect, 2 (21). pp. 5958-5964. ISSN 2365-6549

https://doi.org/10.1002/slct.201701211

© 2017 Wiley-VCH Verlag GmbH & Co. KGaA, Weinheim. This is the peer reviewed version of the following article: L. Jones, C. M. Pask, A. Kazlauciunas, M. Gulcur, L. Lin (2017) ChemistrySelect, 2 (21), 5958-5964, which has been published in final form at https://doi.org/10.1002/slct.201701211. This article may be used for non-commercial purposes in accordance with Wiley Terms and Conditions for Self-Archiving. Uploaded in accordance with the publisher's self-archiving policy.

Reuse

Items deposited in White Rose Research Online are protected by copyright, with all rights reserved unless indicated otherwise. They may be downloaded and/or printed for private study, or other acts as permitted by national copyright laws. The publisher or other rights holders may allow further reproduction and re-use of the full text version. This is indicated by the licence information on the White Rose Research Online record for the item.

Takedown

If you consider content in White Rose Research Online to be in breach of UK law, please notify us by emailing eprints@whiterose.ac.uk including the URL of the record and the reason for the withdrawal request.

eprints@whiterose.ac.uk
https://eprints.whiterose.ac.uk/

Synthesis and Characterisation of Fused-Heterocyclic Molecular Rods: A Combined Experimental and Theoretical Study on Diethynyl-Dithienothiophenyl Derivatives

Leighton Jones[a], Christopher M. Pask[b], Algy Kazlauciunas[c], Murat Gulcur[a]* and Long Lin[a]*

Abstract: A structural and electronic diversity of symmetric ethynyl dithienothiophenyl (DTT) molecular rods were synthesised and their properties fully characterised using optical and thermal analysis and complemented with density functional theory (DFT) calculations. It was found that some structures are stable up to 381 ℃. Due to the nature of both the derivative and the substituent, physical properties such as electron donating ability and thermal stability can be fine-tuned to generate rationally designed materials, all of which have excellent solubility in common organic solvents. The single-crystal x-ray structures revealed that both bulky silyl and linear alkyl derivatives generate regular lateral close packing between the adjacent molecules, suitable for charge-transfer in organic thin-film transistors (OTFTs), whereas the same ethynyl derivative without an alkyl chain gives a non-planar interlinking structure and thus unsuitable for OTFTs. These air-stable electron rich DTT-based molecular rods have strong potential as organic semiconductors for organic electronic applications.

Introduction

The alkyne bond has been realised as an intrinsic functional group due to its propensity for conversion through transformations such as carboxylation[1], hydro-amination[2] and addition to electrophiles[3]. Electron-rich alkyne substrates enable the construction of drug scaffolds[4,5] normally unavailable from conventional synthetic approaches and a number of catalytic systems have been developed to synthesise polycyclic heterocycles from alkynes as enhanced fluorescence probes[6-9]. Single alkynes can furnish heterocycles such as triazoles[10,11], furans[12] and oxazoles[13] while two alkynes in close array can undergo domino reactions to afford poly-fused aromatics[14], thereby yielding complex products from simple building blocks.

A careful selection of the core, capping and fine-tuning units for alkyne molecular substrates[15] is critical for the improvement of physical properties. By structural and heteroatom variation of the derivative, the properties can be fine-tuned for a given application, or used to selectively control the reactivity of the alkyne bond towards further functionalisation. For example, the functionalised products presented in Fig. 1 are structurally diverse but are all derived from the same rod-like substrate. The resulting donor-acceptor structures[3,16], with strongly-conjugated organic substituents, have a number of applications other than medicinal scaffolds and include optoelectronics, photovoltaics, and photonics; partly due to their electron-rich structures but also partly due to their structural diversity, facilitating both non-linear optical (NLO) phenomena and charge-transfer properties[17]. Indeed, their rod-like alkyne substrates have a tendency to promote charge transfer and such intrinsic organic semiconductor behavior is realised as molecular wires and transistors in organic electronics[18].

Some leading examples of molecular rods are shown in Fig. 2, which have thiophene as the central core unit sandwiched between two alkyne derivatives. These structures present the thiophene-based homologous series of diethynyl molecular rods. Naturally, the monothiophenyl molecular rods have been extensively explored in the literature, from alkyl[19] and silyl[19,20] groups through aromatic[19,21,22], heteroatomic aromatic substituents such as pirydyl[23], anisyl[24] and methoxy[25], to bulky aromatic pyrene[26] units. Due to the challenging multi-step synthesis of the next fused-ring homologue, thienothiophene (TT), a limited number of structures are reported and include tertiary-butyl[27], trimethylsilane[27,28], phenyl[22] and phenylthioacetate[29]. Following this trend, the next homologue in the series is dithienothiophene (DTT), which has yet to be fully explored in the literature and is the focus of the present study. To date, there are only a few reports on DTT alkyne derivatives[4,30-32] that present a thorough characterisation of a range of structurally diverse units. These include metallated alkynes such as gold[28], iron[31], platinum[33] and ferrocene[34], while DFT modeling[35,36] was

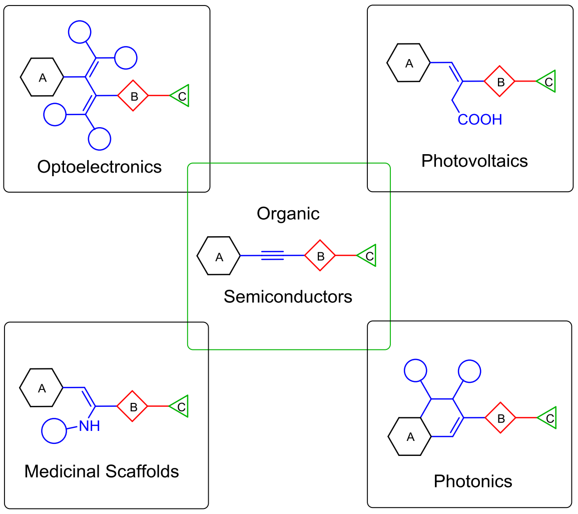

Fig. 1. Modification and application of alkyne substrates; [A] core, [B] end-capping and [C] fine-tuning derivative units.

---

[a] Dr L. Jones, Dr M. Gulcur and Prof. L. Lin*
Centre for Industrial Collaboration, School of Chemistry
University of Leeds, West Yorkshire, UK, LS2 9JT
[b] Dr. C. M. Pask
School of Chemistry, University of Leeds, West Yorkshire, UK, LS2 9JT
[c] Dr A. Kazlauciunas
Colour Science Analytical, School of Chemistry
University of Leeds, West Yorkshire, UK, LS2 9JT
E-mail to L.Lin@leeds.ac.uk, murat@gulcur.com

Supporting information containing experimental, crystallographic and computational data for this article is given via a link at the end of the document.

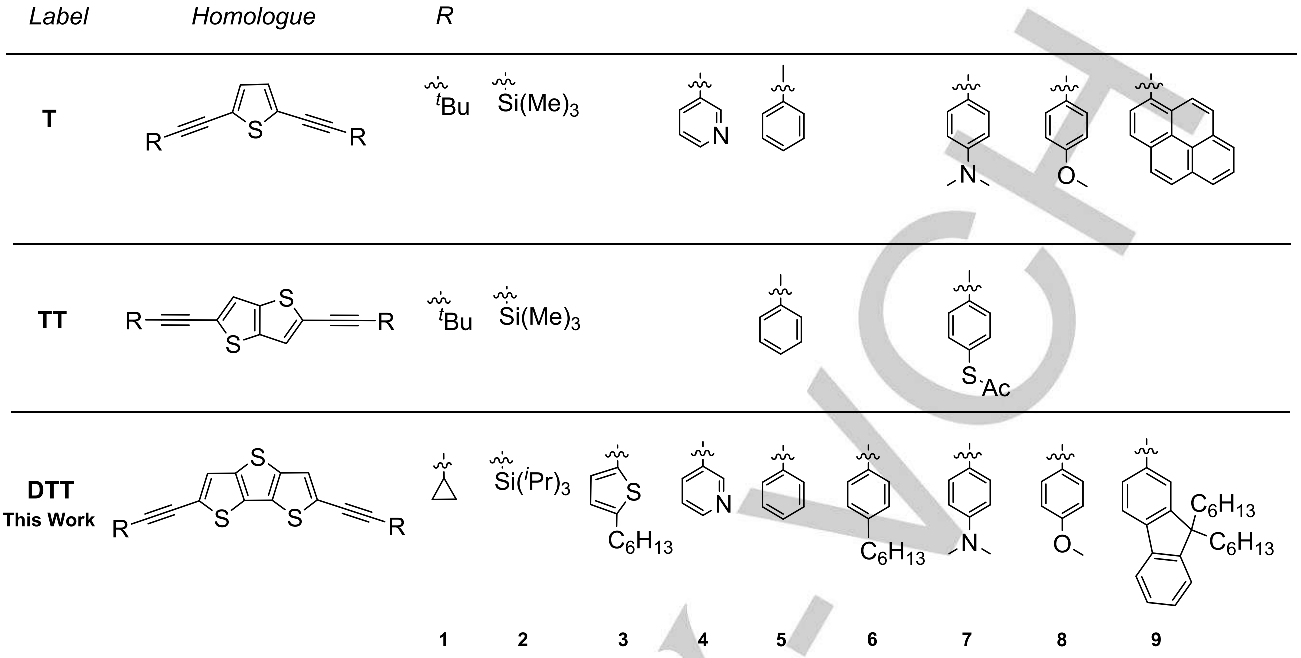

Figure 2. Leading examples of heterocyclic π-extended molecular rods with ethylene spacer units and fused-ring thiophenyl cores. The theoretical structures and physical properties of compounds **2**, **3** and **6** were first reported in reference 32 and **5** in reference 36; herein we report their synthesis and full characterisation.

reported for structures yet to be prepared in the literature, for applications such as molecular wires.

Moreover, DTT core units are known to be highly stable[37,38] and impart closer intermolecular interactions in the solid state that facilitate greater physical properties for electronic device applications. Interestingly, there are no reports on heteroatoms (silicon, nitrogen, oxygen) located at the periphery of the DTT-alkyne moieties. Herein, we present the synthesis and characterisation of organic diethynyl-dithienothiophenyl structures as the next in the homologous series of thiophene-based molecular rods.

Results and Discussion

The synthetic strategy adopted for these molecular rods is the divergent approach, starting with the synthesis of the DTT core and then π-expansion with C-C coupling (Scheme 1). Unfortunately, attempts to include thiazyl and thioanisyl motifs using this strategy were unsuccessful. The alternative strategy devised by Raithby et al.[28] found isolated diethynyl-DTT to be unstable and thus unsuitable for this study. Dibromo-DTT (**16**) was synthesised according to the latest route reported by Holmes et al., which is a facile, high-yielding three-step route starting from commercially available tetrabromothiophene[39]. The derivatised bromide and alkyne reagents were used as bought at high-purity grades (98-99$^+$ %). Compounds **3**, **6** and **9** were synthesised via an initial Sonogashira coupling of a brominated substrate with trimethylsilylacetylene (Scheme 1, A), followed by deprotection with TBAF affording the alkyne[40]. Subsequent addition to **16** using a second Sonogashira reaction (Scheme 1, B) gave the target products in yields of 61-67 %, compared to the TT analogues[22,27-29]. The alkyne derivatives were chosen for their structural and heteroatom variation, while also designed to ensure good solubility, an important factor in solution-processed thin-film transistors[37,38].

Single-crystal X-ray structures[41] of the individual molecules and the unit cell packing for compounds **2**, **5**, **6**, **7** and **8** are presented in Fig. 3; compounds **1**, **3**, **4** and **9** did not crystallise. Compound **2** crystallised in a monoclinic cell and was solved in the I2/a space group, with half a molecule in the asymmetric unit. There is an in-plane bending distortion between the TIPS groups and the DTT course of the single molecular structure. The isopropyl units lock the molecules together into an ideal brick-weave type motif.

The phenyl derivative, compound **5**, crystallised in an orthorhombic cell and solved in the $P2_12_12_1$ space group. The

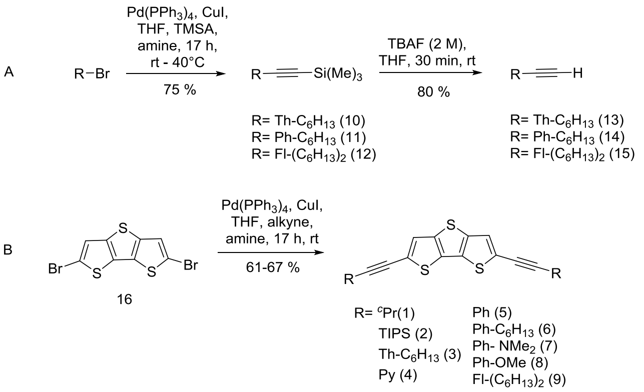

Scheme 1. Synthesis of symmetric dithienothiophenyl ethynyl derivatives under mild Sonogashira conditions using readily available alkynes.

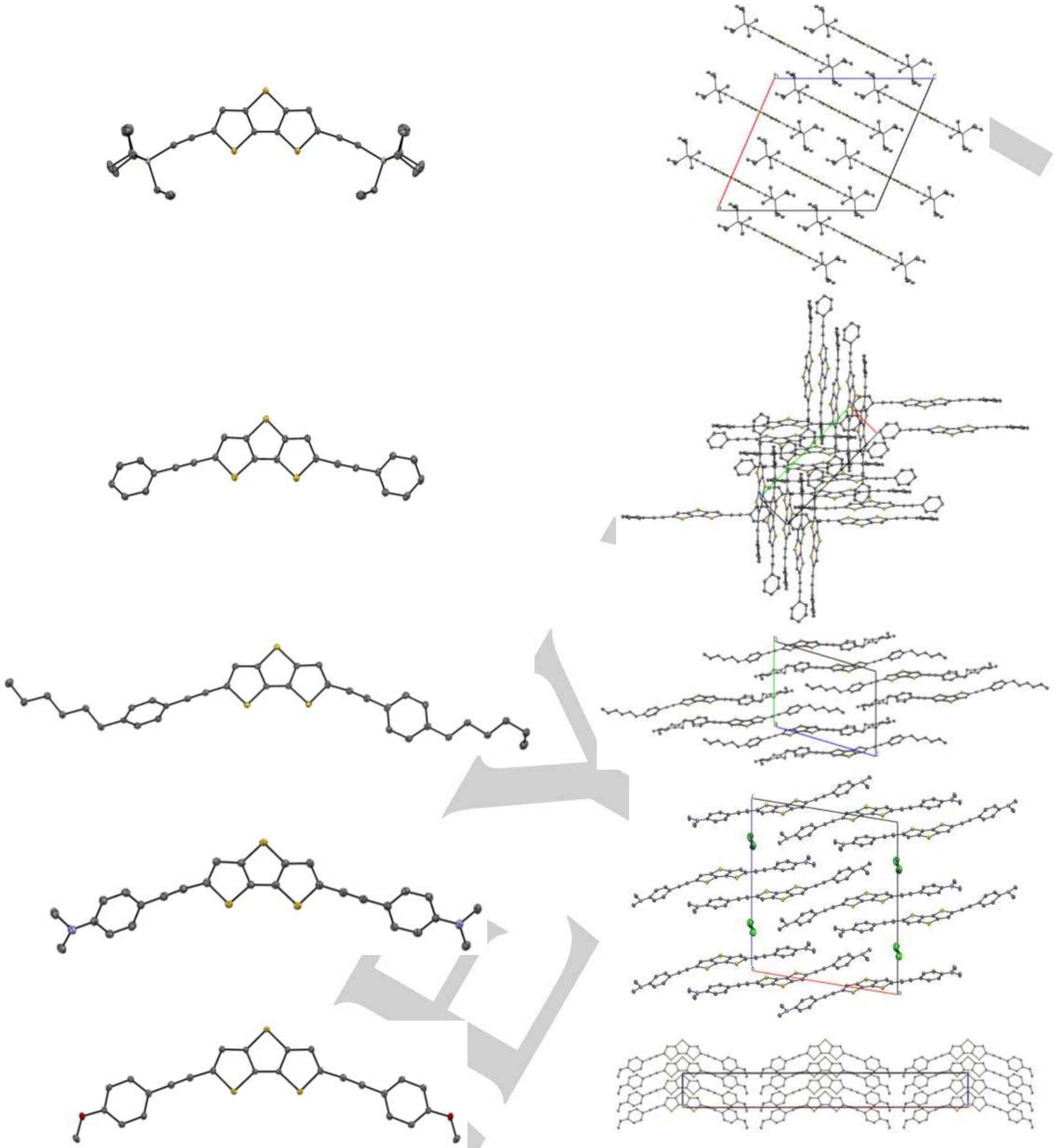

2

5

6

7

8

Figure 3. Single crystal X-ray ORTEP plots with thermal ellipsoids at the 50 % level of the single molecules and their packing in the unit cell for A (TIPS), B (Ph-C_6H_{13}), C (Ph-OMe) and D (Ph-NMe_2); hydrogen atoms removed for clarity.

unit cell is remarkably different from all other crystallised compounds (Fig. 3), due to different layers stacking perpendicular to each other. The phenyl-hexyl derivative **6**, crystallised in a triclinic unit cell and the P-1 space group. The hexyl units stack cooperatively, differing significantly from the unit cell of compound **5**. The phenyl rings of **6** have a herringbone type arrangement along the crystallographic a-axis, with the adjacent molecules bound through S-S (3.400 Å) and S-π (3.213 Å) interactions. The aniline derivative **7** crystallised as yellow-green plates in a monoclinic unit cell in the $P2_1/c$ space group with one molecule in the asymmetric unit from the slow diffusion of hexane into dichloromethane, which remained trapped in the single-crystal in between the layers. The methoxy derivative **8** crystallised under the same conditions as **7** as yellow-green plates in the orthorhombic space group $Cmc2_1$ with half a molecule in the asymmetric unit. Interestingly, both **7** and **8** show remarkable structural distortions, where **7** displays an inflection of curvature across the whole molecule, while **8** exhibits a large out-of-plane bend[42] of 34.7 ° (Fig. 4). This phenomenon suggests these rod-like structures have a relatively high degree of flexibility.

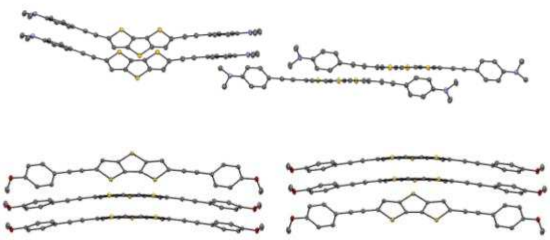

7

8

Figure 4. Single crystal X-ray ORTEP plots with thermal ellipsoids at the 50 % level showing an inflection of curvature across **7** and a large out-of-plane bending distortion with **8**.

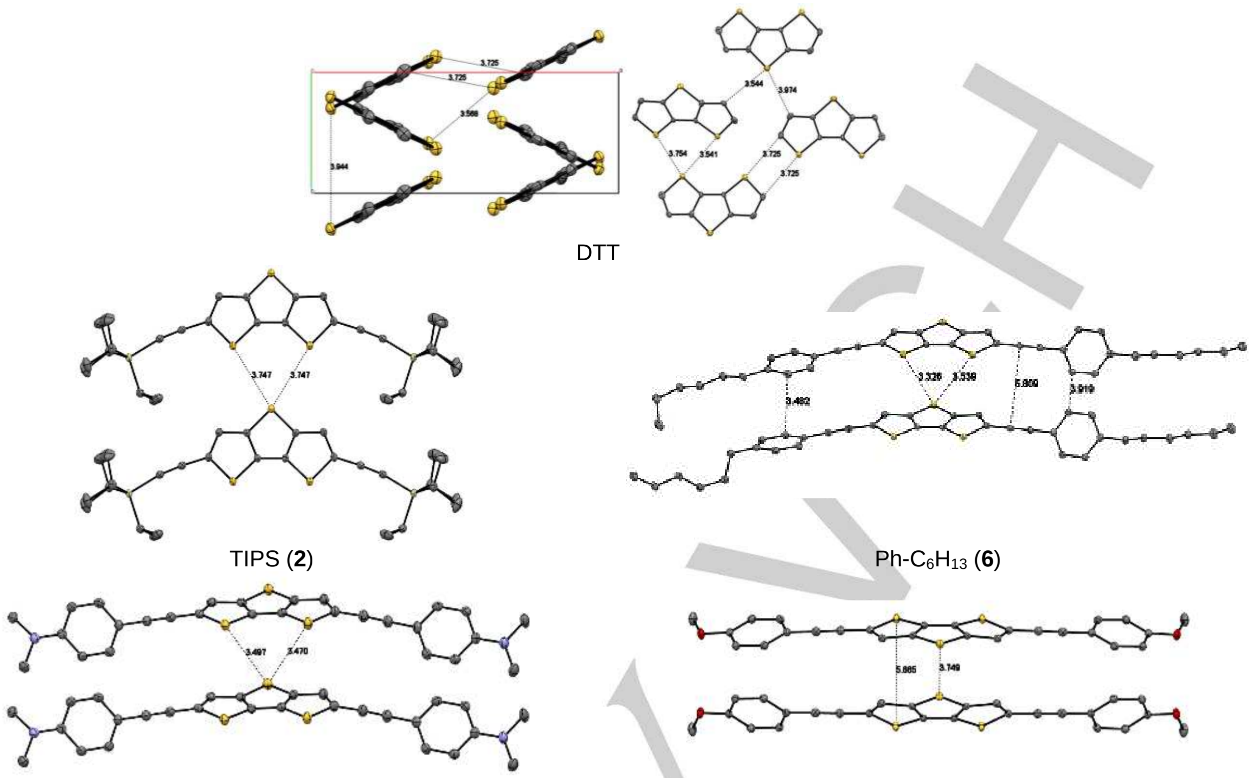

DTT

TIPS (**2**)

Ph-C_6H_{13} (**6**)

Ph-NMe_2 (**7**)

Ph-OMe (**8**)

Figure 5. Single crystal packing of a pure DTT molecule and the compounds **2**, **6**, **7** and **8**, showing the intermolecular distances between the sulfur atoms of the central and outer thiophene rings between the adjacent molecules; presented as single crystal X-ray ORTEP plots with thermal ellipsoids at the 50 % level.

The distances between the adjacent molecules and layers were compared to those in a single-crystal structure of pure DTT. Fig. 5 shows several intermolecular distances between the sulfur atoms of the thiophene rings. The sulfur or carbon atoms of the each thiophene in DTT has intermolecular distances with the corresponding ring or to the adjacent molecule of 3.54-3.75 Å. In comparison, all four of the single-crystal structures presented in this work have very similar intermolecular distances, regardless of the large out-of-plane bends, twisted phenyl rings or solvent incorporation. These distances correlate well with the literature for TT analogues[27,28], suggesting these could be ideal candidates for potential use in organic semiconductors.

Selected structural parameters from the single-crystal data are presented in Table 1; DFT[43] calculations were performed for all compounds and results are available in the SI. The DFT values show exceptional correlation to the single-crystal bond lengths (< 0.02 Å) and angles (< 3 °) and can thus be used with confidence for a reliable structural prediction. The table shows the C2-C6 bond length is less than the C3-C4 bond in DTT, suggesting significant aromaticity concentrated in the central thiophene ring. This is corroborated with the differences between the C-S bonds, such that S5-C6 < S5-C4. The alkyne bonds are noticeably longer for the single-crystal structures **2** and **7** than for **6** and **8**, possibly owing to the strength in their electron donating power and thus slightly weakening the triple bond; the corresponding DFT calculations in the SI‡ for the alkyne bond lengths correlate well, in comparison to the single-crystal data. The bond angle C4-S5-C6 is 91 ° for the terminal thiophene, reproduced across all structures and 111-112 ° for the C=C-C intra-ring angles. The angle C7-C4-S5 between the alkyne bond and thiophene ring varies between 117-119 °, due to the different structural distortion phenomena.

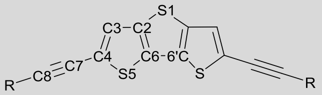

Table 1. Selected bond lengths (Å) and angles (°) from single crystal structures, with estimated standard deviation in parenthesis.

Bond Length	**2**	**5**	**6**	**7**	**8**
S1-C2	1.744(16)	1.746(2)	1.736(15)	1.749(2)	1.744(2)
S5-C6	1.720(16)	1.723(2)	1.716(15)	1.724(2)	1.724(2)
C6-C6’	1.418(3)	1.416(3)	1.418(19)	1.411(3)	1.413(4)
C2-C6	1.384(2)	1.392(3)	1.394(19)	1.388(3)	1.391(3)
C2-C3	1.418(2)	1.409(3)	1.419(19)	1.410(3)	1.415(3)
C3-C4	1.367(2)	1.376(3)	1.369(2)	1.374(3)	1.373(4)
C4-C7	1.424(2)	1.418(3)	1.421(2)	1.410(3)	1.417(3)
C4-S5	1.751(16)	1.756(2)	1.750(14)	1.756(2)	1.752(2)
C7-C8	1.208(2)	1.199(3)	1.202(2)	1.206(4)	1.200(3)
Angle					
C4-S5-C6	90.9(8)	91.3(11)	91.1(7)	91.1(11)	91.1(12)
S5-C6-C2	111.4(12)	110.7(17)	111.3(11)	110.9(17)	110.9(15)
C2-C6-C6’	112.4(9)	112.5(2)	112.1(13)	112.7(2)	112.3(12)
C6-C2-S1	112.4(12)	112.5(17)	112.7(11)	112.0(17)	112.6(16)
C2-C3-C4	111.2(14)	111.4(2)	111.2(12)	111.2(2)	110.9(2)
C7-C4-S5	117.2(12)	119.8(18)	118.3(11)	17.3(18)	118.0(18)

The FMO energy levels for the HOMO and LUMO states are presented in Fig. 6 and include the work function of a gold electrode, one of the most commonly used[44] (-5.1 eV). The silyl (**2**) and pyridyl (**4**) compounds have the lowest HOMO levels at -5.68 and -5.69 eV respectively, whereas the methoxy derivative **8** has the highest (-4.49 eV). The smallest optical energy gaps E_g are with **3** and **7** at 2.89 and 2.90 eV, while the largest is with the cyclopropyl **1** (3.55 eV) and silyl **2** compounds (3.48 eV); the pyridyl **4** and phenyl-based compounds **6**-**8** all have similar gaps between 3.04-3.08 eV. The relatively close energies between the HOMO levels and the work functions for all compounds makes them suitable for OTFT applications[45-47].

The FMOs are plotted in Table 2, and shows relatively little molecular orbitals on the alkyne derivatives of compounds **1** and **2**. Compound **3** has orbitals across all carbon atoms in the thiophene unit, yet **4** and **5** lack orbitals on two atoms of their six-membered ring derivatives. In contrast, compounds **6**-**7** show orbitals on all atoms of the phenyl unit and the methyl, methoxy and dimethylamine units, showing the HOMO state can be π-extended across and beyond the aromatic derivatives. Except for **1** and **2**, all LUMO states for compounds **3**-**9** show extensive orbitals of similar pattern across the breadth of the structures.

The optical properties of the compounds were probed using UV-Vis spectroscopy (Fig. 7) and clearly shows the diversity of their electronic structure. In general, the optical-gap decreases with increasing aromaticity of the derivative, where the silyl **2** has the largest (338 nm) and the dimethylamine derivative 7 has the smallest (468 nm). The split in the absorption peaks of **1** and **2** is not reproduced by the other compounds and although uncommon in the literature, the phenomenon is present for some oligo-fused thiophenes[48]. The pyridyl derivative **4** has an absorption curve that is highly similar to that of compounds **5** and **8**, suggesting there is little difference in terms of electron density or donating and withdrawing power amongst these derivatives. Except for **2**, there is relatively little absorption in the 200-300 nm region, although low-intensity peaks are centered on 300 nm, while other peaks at lower wavelengths centered on 250 nm arising from deep energy levels.

Table 2. Frontier molecular orbital plots of the highest occupied and lowest unoccupied with their energies in electron volts (eV).

Entry	ϵ_H / eV	ϵ_L / eV
1	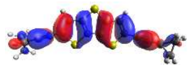 -5.49	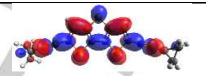 -1.94
2	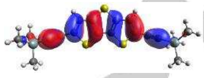 -5.68	 -2.20
3	 -5.23	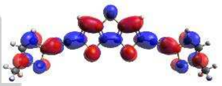 -2.34
4	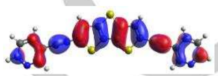 -5.69	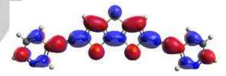 -2.62
5	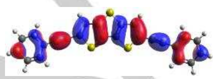 -5.46	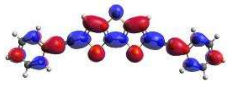 -2.38
6	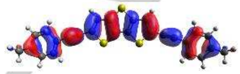 -5.34	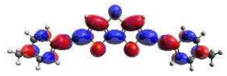 -2.27
8	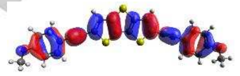 -5.19	 -2.15
7	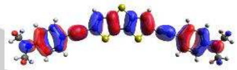 -4.81	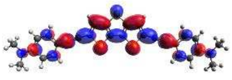 -1.91
9	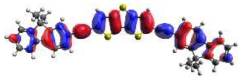 -5.27	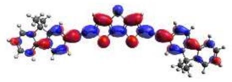 -2.38

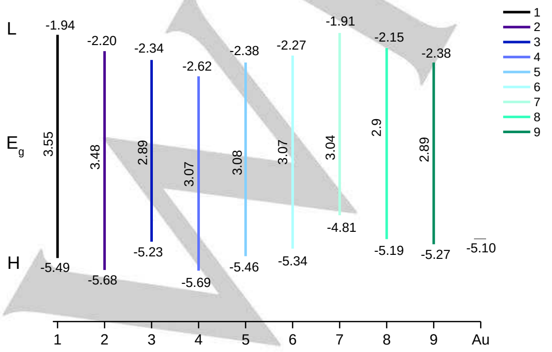

Figure 6. FMO plots (eV) with the work function of a gold electrode

Thermal decomposition profiles were investigated with thermal gravimetric analysis (TGA) as seen in Figure 8. The profiles for most compounds exhibit two thermal decomposition temperatures, with the second onset being around 381 ℃ for all. This common temperature suggests the origin is most likely to be the breakdown of the DTT core unit. All compounds show good thermal stability, with the first decomposition onset of **8** at 60.5 ℃ followed closely by **4** at 73.1 ℃. **1** and **7** are the most stable and decompose much higher around 170 ℃. Interestingly, compound **5** decomposes at 252.7 ℃, whereas compound **6** decomposes at

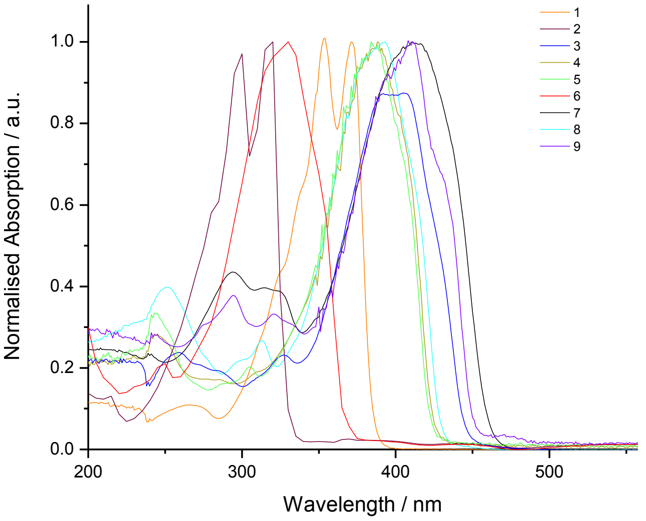

Figure 7. A composite normalised UV-Vis spectra of all compounds, in chloroform at 21 ℃.

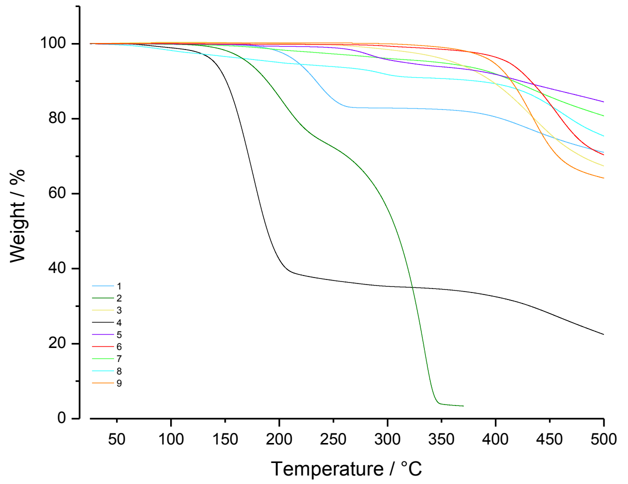

Figure 8. Thermal gravimetric analysis (TGA) of the sample weight (%) under nitrogen between 25 ℃ and 500 ℃.

381.5 ℃, being a 128.8 ℃ difference. This suggest s strong electron donation highly stabilises the alkyne bond and overall structure.

Conclusion

In conclusion, electron rich molecular rods containing a DTT core and capped with a structural variety of derivatised alkynes were synthesised and fully characterised, including optical, electronic, thermal and DFT analysis. It was found that a number of which are highly stable, up to 381 ℃, show close packing suitable for charge-transfer and have excellent solubility in common organic solvents which are perfectly suited to OTFTs. Based on the understanding developed here, highly aromatic π-extended molecular wires are currently under synthesis in our laboratories.

Experimental Section

General procedure for the synthesis of the symmetric dithienothiophenyl ethynyl derivatives: Under nitrogen a flame-dried flask was evacuated and backfilled three times, which was then charged with a solution of 2,2'-dibromodithieno[2,3-b:3',2'-d]thiophene (0.732 g, 2.08 mmol), copper iodide (0.0093 g, 0.048 mmol) and tetrakistriphenylphosphine palladium (0) (0.120 g, 0.104 mmol) in tetrahydrofuran (20 mL) and diisopropylamine (2 mL). The solution was bubbled with nitrogen for 15 min. The selected alkyne (1.00 g, 5.21 mmol) was added dropwise and the mixture stirred for 17 h at room temperature. The mixture was filtered and the solvent evaporated giving a crude residue which was purified with flash column chromatography (40 % dichloromethane in petroleum ether 40-60 ℃) then recrystallised from hexane giving an orange crystalline powder (0.45 g, 62 %).

Acknowledgements

We gratefully acknowledge Gunnell and Matthews Scholarship for financial support. We thank Tanya Marinko-Covell for elemental analysis services at the University of Leeds.

Keywords: alkynes • density functional calculations • fused-ring systems • heterocycles •

1 M. Beesu and M. Periasamy, J. Organomet. Chem., **2012**, 705, 30-33.

2 H. Siebeneicher and S Doye, eur. J. Org. Chem., **2002**, 1213-1220.

3 T. Shoji, S. Ito, K. Toyota, M. Yasunami and N. Morita, Chem. Eur. J., **2008**, 14, 8398-8408.

4 K. A. Leonard, M. I. Nelen, L. T. Anderson, S. L. Gibson, R. Hilf and M. R. Detty, J. Med. Chem., **1999**, 42, 3942-3952.

5 S. Altomonte, G. L. Baillie, R. A. Ross and M. Zanda, RSC Adv., **2015**, 5, 13692-13701.

6 S. Hiraoka, M. Shiro and M. Shionoya, J. Am. Chem. Soc., **2004**, 126, 1214-1218.

7 M. Yamashita, K. Hirano, T. Satoh and M. Miura, Org. Lett., **2009**, 11, 2337-2340.

8 Z. Shi, S. Ding, Y. Cui and N. Jiao, Angew. Chem. Int. Ed.**2009**, 48, 7895-7898.

9 J.-R. Huang, Q.-R. Zhang, C.-H. Qu, X.H. sun, L. Dong and Y.-C. Chen., Org. Lett., **2013**, 8, 1878-1881.

10 V. D. Bock, H. Hiemstra and J. H. Van Maarseveen, Eur. J. Org. Chem., **2006**, 51-68.

11 B. R. Buckley, S. E. Dann, D. P. Harris, H. Heaney and E. Stubbs, Chem. Commun., **2010**, 46, 2274-2276.

12 G. Zeni and R. C. Larock, Chem. Rev., **2004**, 104, 2285-2309.

13 R. Ding, Y. Li, C. Tao, B. Cheng and H. Zhai, Org. Lett., **2015**, 17, 3994-3997.

14 T. Willumstad, P. D. Boudreau and R. L. Danheiser, J. Org.Chem., **2015**, 80, 11794-11805.

15 N. S. Baek, S. K. Hau, H.-L. Yip, O. Acton, K.-S. Chen and A. K.-Y. Jen, Chem. Mater., **2008**, 20, 5734-5736.

16 T. Michinobu, C. Boudon, J.-P. Gisselbrecht, P. Seiler, B. Frank, N. N. P. Moonen, M. Gross and F. Diederich, Chem. Eur. J., **2006**, 12, 1889-1905.

17 F. Nisic, A. Colombo, C. Dragonetti, E. Garoni, D. Marinotto, S. Righetto, F. De Angelis, M. G. Lobello, P. Salvatori, P. Biagini and F. Melchiorre, Organometallics, **2015**, 34, 94-104.

18 a) W. Hong, D. Z. Manrique, P. Moreno-Garcia, M. Gulcur, A. Mishchenko, C. J. Lambert, M. R. Bryce and T. Wandlowski, J. Am. Chem. Soc. **2012**, 134, 2292-2304; b) P. Moreno-Garcia, M. Gulcur, D. Z. Manrique, T. Pope, W. Hong, V. Kaliginedi, C. Huang, A. S. Batsanov, M. R. Bryce, C. Lambert and T. Wandlowski, J. Am. Chem. Soc., **2013**, 135, 12228-12240; c) L. Jones and L. Lin, J. Phys. Chem. A, **2017**, 121, 2804-2813.

19 R. Corriu, T. Deforth, W. Douglas, G. Guerrero and W. Siebert, Chem. Commun., **1998**, 963-964

20 K. Okukara, Bull. Chem. Soc. Jpn., **1981**, 54, 2045-2052.

21 X. Qu, T. Li, P. Sun, Y. Zhu, H. Yang and J. Mao, Org. Biomol. Chem., **2011**, 9, 6938-6942.

22 G. Garcia, J. Granadino-Roldàn, A. Garzón, M. Moral, T. Pana-Ruiz, A. Navarro, M. Fernández-Liencres and M. Fernàndez-Gómez, J. Phys. Chem. C, **2010**, 114, 12325-12334.

23 E. Paegle, S. Belyakov, M. Petrova, E. Liepinsk and P. Arsenyan, Eur. J. Org. Chem., **2015**, 4389-4399.

24 J. Rodríguez, A. Lafuente, L. Rubio and J. Esquirias, Tetrahedron Lett., **2004**, 45, 7061-7064.

25 K. Kishikawa, M. Harris and T. Sweger, Chem. Mater., **1999**, 11, 867-871.

26 R. Mishira and J. Sankar, RSC Advances, **2013**, 3, 10658-10661.

27 K. Asai, G.-li Konishi, Y. Nakajima, S. Kawauchi, F. Ozawa and K. Mizuno, J. Organomet. Chem., **2002**, 653, 46-49.

28 P. Li, B. Ahrens, N. Feeder, P. Raithby, S. J. Teat and M. S. Khan, Dalton Trans., **2005**, 874-883.

29 A. Seidler, J. Svoboda, V. Dekoj, J. Chocholousova, J. Vacek, I. Stará and I. Starý, Tetrahedron Lett., **2013**, 54, 2795-2798.

30 T. Ozturk, E. Ertas and O. Mert, Tetrahedron, **2005**, 61, 11055-11077.

31 H. Shah, R. A. Al-Balushi, M. K. Al-Suti, M. S. Khan, C. H. Woodall, K. C. Molloy, P. R. Raithby, T. P. Robinson, S. E. C. Dale and F. Marken, Inorg. Chem., **2013**, 52, 4898-4908.

32 (i) T. Okujima, A. Toda, Y. Miyashita, A. Nonoshita, H. Yamada, N. Ono and H. Uno, Heterocycles, **2012**, 86, 637-648; (ii) CN105646528A.

33 L. S. Devi, M. K. Al-Suti, N. Zhang, S. J. Teat, L. Male, H. Sparkes, P. R. Raithby, M. S. Khan and A. Kohler, Macromolecules, **2009**, 42, 1131-1141.

34 H. Shah, R. Al.-Balushi, M. Al-Suti, M. Khan, C. Woodall, K. Molley, P. Raithby, T. Robinson, S. Dale and F. Marken, Inorg. Chem., **2013**, 52, 4898-4908.

35 D. Song-Song, Z. Cai-Bin, M. Yan and W. Wen-Liang, Chemical Journal of Chinese Universities, **2013**, 34, 161-169.

36 M. Jothi and P. Kumaradhas, Computational and Theoretical Chemistry, **2012**, 1000, 10-18.

37 C. Wang, H. Dong, W. Hu, Y. Liu and D. Zhu, Chem. Rev.**2012**, 112, 2208-2267.

38 V. Coropceanu, J. Cornil, D. da Silva Filho, Y. Olovier, R. Silbey and J.-L. Brédas, Chem. Rev., **2007**, 107, 926-952.

39 T.-H. Kwon, V. Armel, A. Nattestad, D. R. Macfarlane, U. Bach, S. J. Lind, K. C. Gordon, W. Tang, D. J. Jones and A. B. Holmes, J. Org. Chem., **2011**, 76, 4088-4093.

40 (i) S. Rondeau-Gagné, C. Curutchet, F. Grenier, G. Scholes and J.-F. Morin, Tetrahedron, **2010**, 66, 4230-4242; (ii) S. Ponomarenko and S. Kirchmeyer, J. Mater. Chem., **2003**, 13, 197-202.

41 CCDC contains the supplementary crystallographic data (1537579-1537584) for this paper. These data can be obtained free of charge from The Cambridge Crystallographic Data Centre.

42 J. Siddle, R. Ward, J. Collings, S. Rutter, L. Porrès, L. Applegarth, A. Beeby, A. Batsanov, A. Thompson, J. Howard, A. Boucekkine, K. Costuas, J-F. Halet and T. Marder, New J. Chem., **2007**, 31, 841-851.

43 R. Sanchez-Carrera, V. Coropceanu, D. da Silva Filho, R. Friedlein, W. Osikowicz, R. Murdey, C. Suess, W. Salaneck and J.-L. Brédas, J. Phys. Chem. B, **2006**, 110, 18904-18911.

44 (i) K. Heard, J. Morrison, L. Weston, C. Lo, L. Pirvu, J. Raftery, M. Little, J. McDouall, S. Yeates and P. Quayle, Chem. Commun., **2015**, 51, 6115-6118; (ii) T. Yamamoto and K. Takimiya, J. Am. Chem. Soc., **2007**, 129, 2224-2225; (iii) H. Klauk, U. Zschieschang, R. Weitz, H. Meng, F. Sun, G. Nunes, D. Keys, C. Fincher and Z. Xiang, Adv. Mater., **2007**, 19, 3882-3887; (iv) R. Chesterfield, J. McKeen, C. Newman, P. Ewbank, D. da Silva Filho, J.-L. Brédas, L. Miller, K. Mann and C. Frisbie, J. Phys. Chem. B, **2004**, 108, 19281-19292.

45 V. Huong, T. Tai and M. Nguyen, Phys. Chem. Chem. Phys., **2012**, 14, 14832-14841.

46 C. Newman, C. Frisbie, D. da Silva Filho, J.-L. Brédas, P. Ewbank and K. Mann, Chem. Mater., **2004**, 16, 4436-4451.

47 C. Wang, Z. Wei, Q. Meng, H. Zhao, W. Xu, H. Li and W. Hu, Org. Electron., **2010**, 11, 544-551.

48 M. Cinar and T. Ozturk, Chem. Rev., **2015**, 115, 3036-3140.

Entry for the Table of Contents (Please choose one layout)

Layout 1:

COMMUNICATION

Text for Table of Contents

((Insert TOC Graphic here))

Author(s), Corresponding Author(s)*

Page No. – Page No.

Title

Layout 2:

COMMUNICATION

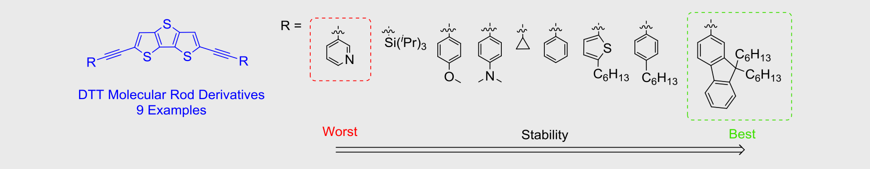

DTT-based molecular rods comprised of heteroatomic and heterocyclic derivatives have surprising single-crystal structures and stabilities. Flexibility in the solid state is observed with some having remarkable out-of-plane deformations, yet retain a close-packed unit cell. The functional group was found to significantly affect both packing and stability, with the most stable being the alkyl-substituted aromatic derivatives, with potential applications in organic thin film transistors (OTFTs).

Leighton Jones, Dr. Christopher Pask, Dr. Murat Gulcur*, Dr Algy Kazlauciunas, Prof. Long Lin*

Page No. – Page No.

Synthesis and Characterisation of Fused-Heterocyclic Molecular Rods: A Combined Experimental and Theoretical Study on Diethynyl-Dithieothiophenyl Derivatives